Chapter 2
Intelligent Control System for High Speed Machining

Antonio Jr. Vallejo Guevara[1], Ricardo A. Ramírez Mendoza[1] and Ruben Morales-Menendez[1]

Abstract The next-generation of high-speed machining (*HSM*) systems demand advanced features such as intelligent control under uncertainty. This requires, in turn, an efficient administration and optimization of all system's resources towards a previously identified objective. This research project presents an optimization system based on Markov decision process (*MDP*), where an intelligent control guides the actions of the operator in peripheral milling processes. The system bases its decisions on prediction models of the machining process: state of wear of the cutting tool and surface roughness; therefore, an estimator based on multi-sensors and data fusion will be analyzed. Exploiting intensive experimentation, databases, models, and detailed procedures generates high precision models. The initial results and the continuous development based on machine learning (*ML*) for *MDP* demonstrate great expectations of this proposal.
Keywords: Markov decision, Process optimization, High speed machining, Milling process, Artificial neural networks

2.1 Introduction

HSM requires high magnitudes of spindle speeds, feed rates, as well as high acceleration and deceleration rates. Simultaneously, it is subjected to stringent restrictions such as low machining cost and time, and high precision and accuracy. Intelligent machines can meet the strong competitiveness demanded by new businesses. Intelligent *CNC* machines convey advanced features such as prediction of operations, reduction of setup time, detection of cutting tool condition, acquisition of knowledge, and inferences from incomplete information Balic (2006). However, process planners still have great difficulties for measuring *on-line* process data on machining processes such as cutting tool wear condition (*CTWC*) and surface roughness (*Ra*) Jawahir and Wang (2007). An intelligent control system for *HSM* is described, exhibiting several desirable features such as: prediction of key variables (*Ra* and *CTWC*), definition and adaptation of optimal cutting conditions and operation policy, and an objective function-based optimization. Special emphasis is placed on *Ra* and *CTWC* modeling due to the resurgence of some *ML* algorithms, the Industry 4.0 and the industrial Internet of things (*IIoT*). A novel mathematical framework for fault diagnosis

[1]Tecnológico de Monterrey, Av. E. Garza Sada # 2501 , e-mail: avallejo@tec.mx, ricardo.ramirez@tec.mx and rmm@tec.mx

(i.e. cutting tool wear condition and surface roughness) is proposed as a key support of intelligent control under uncertainty for *HSM* systems.

2.2 State of the Art

2.2.1 High-Speed Machining

Several optimization methods have been developed around process planning systems for machining processes. For example, a procedure for tool selection in milling operations was proposed in Carpenter and Maropoulos (2000). First, several alternatives of cutting tools were considered by an iterative method. Then, cutting data was refined by a set of technological constraints, including tool life, surface finishing, machine power, and available spindle speeds and feed rates. Finally, three user-defined optimization strategies were available (minimum cost, maximum production rate, or predefined tool life).

In Dereli et al. (2001), a cutting parameters optimization system, based on a two-stage methodology, was introduced. First, a tentative number of passes and depth of cuts were determined through the so-called volume sectioning method. Then, the cutting speed and feed rate for each pass were optimized by using genetic algorithms (*GA*). A second-order mathematical model was developed for predicting the parameter *Ra* as a function of the cutting speed, feed rate, depth of cut, and nose radius of the cutting tool in turning operations Suresh et al. (2002).

Based on previous work by Dereli et al. (2001), an algorithm for the selection of optimal cutting conditions was proposed in Mursec and Cus (2003), allowing the calculation of several cuts required and machining time. Zuperl et al. (2004) presented a new hybrid optimization technique based on the maximum production rate criterion and ten technological constraints. A general algorithm, called *OPTIS*, was used in conjunction with artificial neural networks (*ANN*) to solve the complex optimization problem. *OPTIS* selects the optimum cutting conditions (based on minimum machining costs) from commercial databases. *ANN* ensured an efficient and fast selection of the optimum cutting conditions and processing of available technological data. Compared to the *GA* and linear programming approaches, this hybrid optimization technique improved the optimal cutting parameters selection by around 30.41% and 20%, respectively. Based on *OPTIS*, Zuperl et al. (2006) proposed an adaptive neural controller for on-line optimal control of a milling process.

A two-phase optimization strategy based on the *Taguchi* dynamic characteristic theory was proposed in Tzeng and Chen (2005). Experimental results showed that the machining time could be reduced with low process variance and increased robustness of the *CNC* milling processes.

Yih-Fong (2005) presented a *Taguchi* method coupled with principal component analysis for the optimization of *HSM* milling processes. Optimal process conditions were selected for producing the best dimensional precision and accuracy, *Ra*, and *CTWC*. The selected control factors were: milling type, cutting speed, feed per tooth, film material, tool material, number of teeth, rake angle, and helix angle. Based on the cutting parameters optimization system an index for the inter-correlated multiple performance features of a *HSM* milling process was computed, obtaining optimized settings.

A genetically optimized neural network system that selects the optimal cutting conditions for milling processes was proposed by Tansel et al. (2006). *GA* was used to maximize the rate of metal removal and minimize the *Ra* based on different *ANN* models. A mathematical model based on both material behavior and machine dynamics were described in Palanisamy et al. (2007).

Mukherjee and Ray (2006) reviewed different optimization techniques in metal cutting processes, discussing a general framework. Reviewed optimization methods currently applied were: *Taguchi* method, response surface methodology (*RSM*), *Mathematical Iterative Search Algorithm*, *GA*, and simulated annealing methods.

In Kant and Sangwan (2014) the authors presented a multi-objective predictive model for the minimization of power consumption and *Ra* during the machining of *AISI 1045* steel. The predictive model used grey relational analysis coupled with principal component analysis and response surface methodology *RSM*. The statistical significance of the proposed predictive model has been tested by the analysis of variance. The obtained results indicate that feed is the most significant parameter followed by the depth of cut and cutting speed to reduce power consumption and *Ra*. The results provide an improvement of 6.59% in power consumption and 2.65% in *Ra* over the best experimental run.

In Karabulut (2015) milling tests were performed based on the *Taguchi DoE* method using *L18* orthogonal array and determined the optimal cutting parameters for *Ra* and cutting force. The analysis results showed that material structure was the most effective factor on *Ra* and feed rate was the dominant factor affecting cutting force. *Ra* values were significantly improved by between 196% and 312% in milling Al_2O_3 particle-reinforced *Aluminum* alloy composite compared to *AA7039* Aluminum. *ANN* was able to predict the *Ra* and cutting force with a *MSE* equal to 2.25% and 6.66%.

In Karkalos et al. (2016) models for the prediction of the *Ra* in milling of *Ti-6Al-4V ELI Titanium* alloy were developed. A set of experiments based on *Box Behnken Design* for a three factor and three level central composite design concept was conducted. Depth of cut, cutting speed and feed rate were selected as input parameters and *Ra* was measured as output. The *MSE* and the correlation coefficient were determined to be 8.6×10^{-3} and $R^2 = 0.97$, respectively; for *ANN* models were 2×10^{-3} and $R^2 = 0.98$, for the test group of the optimum model. Almost all of the previous works are usable within narrow operating conditions only.

In Yang et al. (2019), the authors developed an integrated prediction model based on trajectory similarity and support vector regression, which can predict the tool wear and life. The time domain and wavelet analysis are carried out. Five eigenvectors were selected as the input vectors of the prediction model by studying the correlation between 45 characteristic quantities and the tool wear. The relative errors of flank wear value prediction accuracy in the stable stage of the sample tool were above 88% and the prediction accuracy of the stable stage of Tool 1, 2, and 3 was 88.5%, 87.5%, and 90.5% respectively, by using this integrated prediction model. In Hoang et al. (2020), the authors presented an intelligent control system for self-adjusting on-line cutting condition for *HSM* by considering the tool-wear amount to keep the machined product's quality in allowable limit. The empirical analysis of variance and *ANN* were used. The analysis of variance was used for generating the empirical functions which were used as the boundary condition as well as constraint evaluation. The *ANN* was used for generating the new optimal cutting condition.

2.2.2 Surface Roughness (Ra) Modeling

Surface roughness (*Ra*) has been subject of research for years where four major approaches have been pursued Benardos and Vosniakos (2003): (i) Machining theory; (ii) Experimental investigation; (iii) Design of experiments (*DoE*); and (iv) Artificial intelligence (*AI*), a brief review of these is presented next.

Machining theory. It considers geometric and analytical modeling. Geometric modeling is based on the geometrical motion of a metal cutting process regardless of the cutting dynamics. Some geometric models for turning operation are shown in Boothroyd and Knight (2006). In Lee et al. (2001), a geometric model and a simulation algorithm were developed, calculating cutting parameters, cutter and work-piece geometry, vibration signals, and run-out parameters. Finally, Sai and Bouzid. (2005) used an experimental design with two factors (cutting speed and feed per tooth) and five levels to validate the *Ra* model.

Experimental investigation approach. It requires a full range of experiments handling the most relevant factors, and the results are used to investigate the effect on the observed quality characteristic. In Barber et al. (2001), the *Ra* was computed as a quadratic function of tool service time, and the major parameters involved were tool geometry and *CTWC*. In Abouelatta and Madl (2001), mathematical models for predicting *Ra* were derived based on cutting parameters and vibration signals.

Design of Experiments (*DoE*) approach. The *RSM* and *Taguchi* techniques for *DoE* are the most widespread methodologies for *Ra* prediction. In Ozcelik and Bayramoglu (2006), a statistical model was used for estimating *Ra* in high-speed flat milling, where the parameters involved were the total machining time, depth of cut, step over, spindle speed and feed rate. Similar works are presented in Abouelatta and Madl (2001), Özel and Karpat (2005) and Morales-Menendez et al. (2005). In Subramanian et al. (2014) a mathematical model was developed to predict the *Ra* in terms of machining parameters such as radial rake angle, nose radius of cutting tool, spindle speed, feed rate and axial depth of cut. The authors applied the *RSM* to define the *DoE*; the *Ra* was computed with a second-order quadratic model, which was obtained by applying a regression procedure.

Artificial Intelligence approach. *ANN*, *GA*, Bayesian networks (*BN*) and Fuzzy Logic are typical approaches used in *Ra* prediction. In Azouzi and Guillot (1997) the *ANN*, statistical tools, and sensor fusion techniques were combined to estimate *Ra* and dimensional deviations during turning process (on-line). The *DoE* considered the following factors: feed, speed, depth of cut, coolant, tool wear, and material properties. A surface recognition system for *Ra* prediction was proposed by Tsai et al. (1999), where an *ANN* model was built by using the spindle speed, feed rate, depth of cut and the vibration average per revolution. Also, in Benardos and Vosniakos (2003) it was presented an *ANN* model able to recognize *Ra* in a face-milling process.

In Khorasani and Soleymani-Yazdi (2017), a general dynamic *Ra* monitoring system in milling operations was developed. Based on the experimentally acquired data, the milling process was simulated. Cutting parameters (i.e., cutting speed, feed rate, and depth of cut), material type, coolant fluid, X and Z components of milling machine vibrations, and white noise was used. First neural milling process model was developed with 6 inputs, 12 neurons in hidden layers and 3 outputs. The neural milling process model was used to estimate two components of vibrations and *Ra*. Later, a neural simulator model was developed with 7 inputs, 14 neurons in hidden layers and 1 output, and it was used to predict *Ra*. The average correlation factor was computed for training/testing steps: 99% and 99.7% respectively.

Wu and Lei. (2019) proposed an *ANN* model to predict the *Ra* of *S45C* steel in milling process. The input features to the *ANN* model were feed per tooth, cutting depth, clamping torque of vise, the removed volume accumulation, and the extracted features from the vibration signals (*RMS*, kurtosis, skewness, and the envelope signals on the three-axis).

2.2.3 Cutting Tool Wear Condition (CTWC) Modeling

Monitoring the *CTWC* is very important in all metal cutting processes. There are two monitoring systems: direct and indirect. Direct monitoring systems are not easily implemented because they need ingenious measurement methods. Therefore, indirect measurements are required for the estimation of the *CTWC*, and different sensors must be used for monitoring and diagnosing the *CTWC*. There are important contributions to assess the *CTWC* by applying indirect methods: *ANN*, *BN*, and hidden Markov Models (*HMM*).

Artificial Neural Networks. *ANN* are well known as pattern recognition engines and robust classifiers. *ANN* has been used successfully to combine inputs from multiple sensors for *CTWC*. In Haber and Alique (2003) was developed an intelligent supervisory system for *CTWC* prediction using a model-based approach. First, an *ANN* model was trained considering the cutting force, the feed rate, and the radial depth of the cut. Secondly, the residual error obtained from the measure and predicted force was compared with an adaptive threshold to estimate the *CTWC*. This condition was classified as new, half-worn, or worn cutting tool.

In Saglam and Unuvar (2003), the authors worked with multilayered *ANN* for the monitoring and diagnosis of the *CTWC* and *Ra*. The obtained success rates were of 77% for tool wear and 80% for *Ra*.

In Javed et al. (2012) an improved-extreme learning machine (*Imp- ELM*) algorithm was developed for predicting the *CTWC* of a high-speed *CNC* machine. The *ELM* approach was evaluated using the force-based approach to build a prediction model. The implemented *ANN* architecture in the *Imp-ELM* approach was defined by four inputs, 15 to 25 neurons in the hidden layer, and one neuron in the output layer. The experimentation was made in a high-speed *CNC* milling machine, the work-piece material was Inconel-718, and three cutting tools of tungsten carbide with 6 mm ball-nose/3-flutes were used in the milling operation. The result was not good enough when the unknown data was presented.

In Escajeda-Ochoa et al. (2019) a new proposal for monitoring the *CTWC* was developed by using *ANN* with autoencoders. The recorded signals (vibration, cutting forces, and autoencoders during the machining of aluminum workpieces were pre-processed to obtain the *MFCC*. The raw signals were recorded during the machining process by using four *CTWC*: *New, Half-New, Half-Worn and Worn*. The processed features of the process signals were used to build a stacked space autoencoders neural network. During the training of the *ANN*, important parameters that define the sparsity, regularization, and impact of the sparsity regularizer were adjusted to achieve optimal training avoiding the under-fitting and over-fitting. The proposed methodology allows identification of *TWC* with an accuracy of 99.63%.

In Guo et al. (2022), a novel Multi-scale Pyramid Attention Network (*MPAN*) was proposed which can not only accurately monitor tool wear, but also access the interpretability from aspect of model design and feature extraction. The *MPAN* was constructed according to the periodic characteristic of the two sensory signals, cutting force and vibration, which improves the ability to characterize multiple frequency bands and maintains the periodic meaning of the features to a large extent. The *MPAN* consists of following components: dual-frequency decomposition, dual-frequency attention, pyramid attention and multi-layer perceptron. In two *HSM* experiments with multiple milling conditions, the mean absolute prediction error of *MPAN* was 3.8% and 11.2% respectively, which shows robustness against tool types, milling parameters, and time-varying signals.

Bayesian Networks. *BN*, also known as belief networks, belong to the family of probabilistic graphical models. *BN* combine principles from graph theory, probability theory, computer science, and statistics. In Dey and Stori (2004), a monitoring and diagnosis approach based on a *BN* was presented. This approach integrates multiple process metrics from sensor sources in sequential machining operations to identify the causes of process variations. It provides a probabilistic confidence level of the diagnosis. The *BN* was trained with a set of 16 experiments, and the performance was evaluated with 18 new experiments. The *BN* diagnosed the correct state with a 60% confidence level in 16 of 18 cases.

Abellán et al. (2006) proposed an indirect monitoring multi-sensor system for both *Ra* and *CTWC* using *BN* techniques. In Allen (2006) a *CTWC* monitoring system for milling operation was developed based on the current signal of the spindle motor as the fault indicator signal. Wavelet time-frequency analysis method was employed for the signal processing step. Gaussian process regression, support vector regression, Bayesian rigid regression, nearest neighbor regression, and decision tree methods were implemented to learn a model between tool wear behavior and signal indicators. The decision tree method and Bayesian rigid regression algorithms showed accurate results with accuracy of up to 91.6% for *CTWC* with a promising ability to tolerate and work under changing operating conditions.

Hidden Markov Models. These models are referred to as Markov sources or probabilistic functions of Markov chains. *HMM*s have proved to be indispensable for a wide range of applications in such areas as signal processing, bioinformatics, image processing, linguistics, and others, which deal with sequences or mixtures of components.

In Atlas et al. (2000), the authors used *HMM*s for the evaluation of tool wear in milling processes. The feature extraction from vibrations signals was the root mean squared, the energy, and derivative. Two *CTWC* were defined: worn and no-worn condition. The reported success was around 93%.

Fish et al. (2003) proposed a *HMM*-based classifier that models the dynamics of cutter wear and the dynamics within a cutting pass in a milling application. Each *HMM*s state corresponds to a range of wear, allowing to produce a quantized estimate of cutter wear.

A proposal to exploit speech recognition frameworks in monitoring systems of the *CTWC* was presented in Vallejo-Guevara et al. (2005). Also, Vallejo et al. (2006) introduced a new approach for online monitoring the *CTWC* in face milling. The proposal was based on a continuous *HMM*s classifier, and the feature vectors were computed from the vibration signals between the cutting tool and the workpiece. The feature vectors consisted of the mel frequency cepstrum coefficients (*MFCC*); the success to recognize the *CTWC* was 99.86% and 84.55%, for the training/testing dataset.

The main contributions of this research are:

- The models that predict *Ra* and *CTWC* consider five aluminum alloys widely used in the aeronautical and automotive industries. The models reported in the consulted research usually use a single material.
- In the works reported for milling operations, the *DoE* only considers straight paths or face milling. This work includes a new parameter that allows defining concave, convex, and straight paths, which are common in peripheral milling operations of molds and a great diversity of parts.

- Regarding the *CTWC*, the research only reports two tool wear conditions (new, worn) for a specific tool geometry. The models that predict the *CTWC* consider four states of tool wear and are evaluated for five different diameters of end millings.
- Finally, the intelligent control system allows predicting the cutting parameters (off-line) to obtain the desired *Ra*, considering the different materials and tools. In *HSM*, it is difficult to have a database with recommendations for specific cutting parameters. Usually, they are determined by trial and error.

2.3 Experimental Set Up

Experiments were carried out in an industrial *HSM* center the HS-1000 Kondia, featuring a 25 KW drive motor, 3 axis, 24,000 rpm maximum spindle speed and a Siemens Open Sinumerik 840D controller, and several sensors were installed in the *CNC* machine as shown in Figs. 2.1- 2.2.

Two data acquisition boards acquired the signals with sample rates of 40,000 and 1,000,000, respectively. A milling process was carried with different aluminum alloys, several cutting tools 25^o helix angle, and 2-flute, Sandvik Coromant and several geometries (concave, convex or straight path), Fig. 2.2. Table 2.1 defines the variables and their description used in the *DoE*.

Table 2.1: Definition of variables

Variable	Description	Variable	Description
V_f	Feed rate	HB	Brinell Hardness
n	Spindle speed	*Ra*	Surface roughness
ap	Axial depth of cut	Ra^p	Predicted *Ra*
ae	Radial dept of cut	Ra^d	Desired *Ra*
Curv	Curvature of the geometry	V_B	Flank wear in cutting tools
D_{tool}	Cutting tool diameter	C_c	Cutting conditions: n, V_f, ap, ae
f_z	Feed per tooth	P_c	Cutting parameters (cutting tool, workpiece hardness, etc)
F_y	y-axis workpiece cutting force	P_G	Geometric parameters (cutting tool, path of the cutting process).

2.4 Experimental Database

Most research work related to *Ra* and *CTWC* only considers a specific combination of tool and workpiece material. However, several authors have pointed out the importance of building databases with different materials, cutting tools, and a broader domain in the machining process. In the mold/die industry, the peripheral milling process is a crucial cutting process; the geometric path can be defined as a simple straight line, concave, or convex curvature. Furthermore, in the aeronautic and automotive industries, different aluminum alloys are used according to multiple requirements and applications of the workpieces.

The several groups of factors that affect *Ra* must be considered. The first group is the cutting conditions (cutting speed, feed rate, axial depth of cut, etc.); the second group is the geometry of the cutting

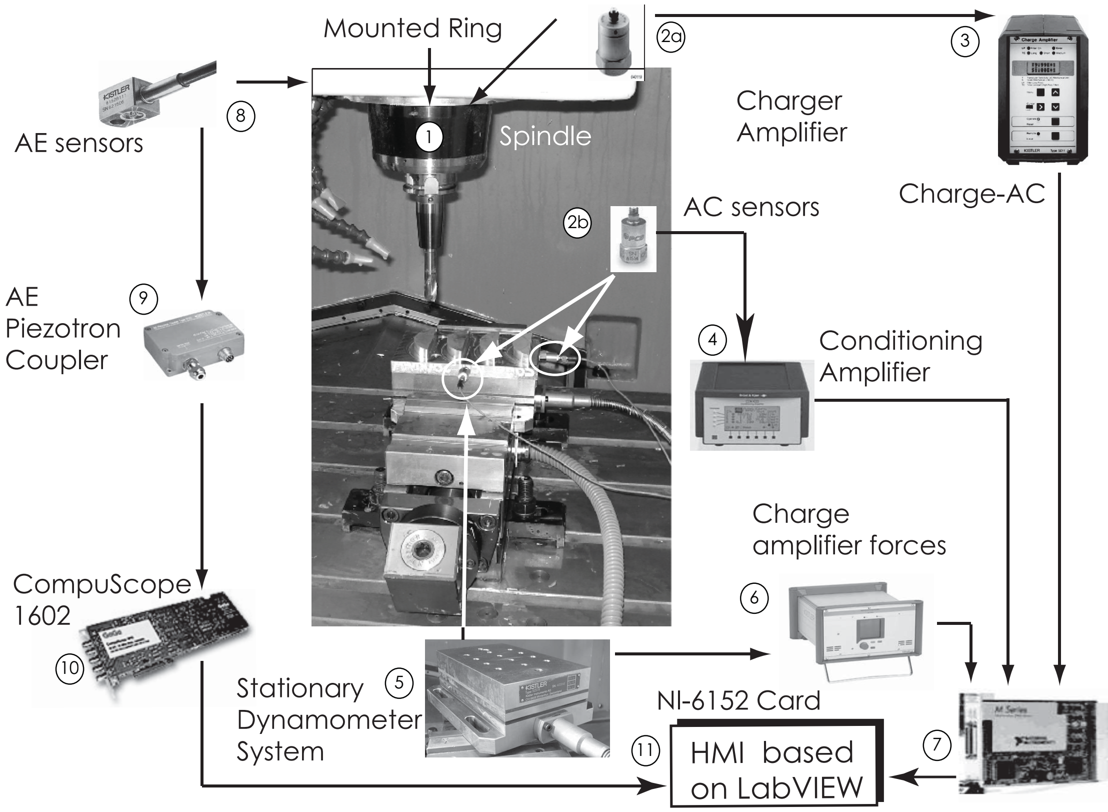

Fig. 2.1: Data acquisition system. The monitoring system is integrated by: (1) Supporting ring, (2a) Brüel & Kjaer accelerometers (charge sensitivity: 98 $+/-$ 2 pC/g, resonant frequency: 16 KHz & 42 KHz), (2b) PCB piezotronic accelerometers (x-axis & y-axis, sensitivity: 10 mV/g; range frequency: 0.3520,000 Hz), (3) Charger amplifiers, (4) Conditioning amplifier, (5) Kistler 3-component forces Dynamometer (force range: -7.5 pC/N in x-axis and y-axis and -3.5 pC/N in z-axis, natural frequency: 3-5 KHz), (6) Kistler charger amplifier, (7) *NI* data acquisition card, (8) Kistler Piezotron *AE* (sensitivity: 700 V/m/s, freq. range: 50-400 KHz), (9) *AE* Piezotron coupler. (10) CompuScope card, and finally, (11) a *HMI* based on *LabView* for real time control and monitoring operations was developed.

tool (tool, diameter, helix angle, edge radius, number of flutes, etc.); the third group is the work-piece material (hardness, ductility, etc.) and path of the peripheral milling process (concave, convex or straight path); the last corresponds to the uncertainty of the process due to the variations in machine vibrations and repeatability, work-holding devices, and other factors. Other variables are less critical or can be controlled (coolant, thermal conditions, humidity, and so on).

A process characterization (screening) design was required in the first experimental stage to compute the critical variables that affect the *Ra*. The *DoE* was calculated by considering eight factors, two levels, 1/8 fraction, 32 runs, zero center points, and four replicates. The selected factors and levels are shown in Table 2.2.

The next step is to apply an analysis of variance for analyzing the significance of factors and/or model terms that address the multiplicity of the tests with the experimental results. The final factors that were

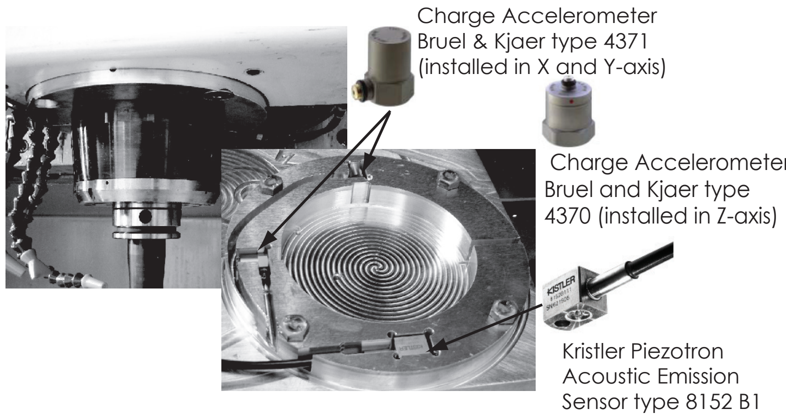

Fig. 2.2: Accelerometers and *AE* sensors installed on a ring fixed to the spindle of the *CNC* machining center.

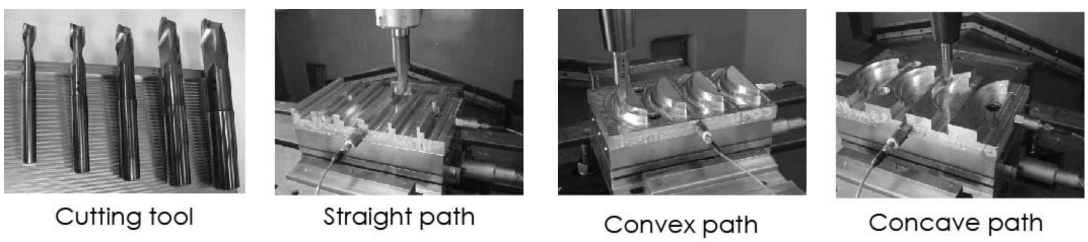

Fig. 2.3: Cutting tools (Sandvik Coromant 8,10,12,14,16 mm) and several geometries (concave, convex, and straight path).

Table 2.2: Factors and levels are defined for the screening design.

Factors	Low level	High level	Units
f_z	0.04	0.13	mm/rev/tooth
V_c	500	850	m/min
ap	5	10	mm
D_{tool}	12	16	mm
ae	1	5	mm
HB	65	145	HB
R	20	40	mm
I/C	Convex	Concave	dimensionless

selected from this analysis are: f_z, D_{tool}, ae, HB, R, and I/C. The last two factors are fused into a new factor called curvature (*Curv*). This factor is computed as the inverse of the radius of the work-piece geometry, and the curvature type is defined by its sign: positive for the convex path and negative for the concave path.

Then, *RSM* is applied to define the runs of the experiments. *RSM* is recommended for modeling and analyzing models with several factors that significantly influence a response. It is based on the central composite design for the design of experiment matrices (Allen, 2006; Montgomery, 2001). Central composite design consists of a 2^{k-1} fractional factorial of resolution with n_F runs and n_c center runs. The defined parameters to apply *RSM* were the following: rotatable central composite design, with 16 points (2^{k-1} = 16, k = number of factors) on cube, 10 points outside of cube, six central points, α = 2 as the radius of the sphere, 32 runs, and four replicates. Table 2.3 shows the factors and levels for the experiments.

Table 2.3: Factors and levels of the experimentation with *RSM*

levels	f_z $\frac{mm}{rev}$	D_{tool} mm	ae mm	HB HBN	$Curvature$ mm^{-1}
-2	0.025	8	1	71	-0.05
-1	0.05	10	2	93	-0.025
0	0.075	12	3	110	0
1	0.1	16	4	136	0.025
2	0.13	20	5	157	0.05

The selected aluminum alloys were: 5083-H111, 6082-T6, 2024-T3, 7022-T6, and 7075-T6. The cutting tool diameters (Sandvik Coromant) were: 8, 10, 12, 16, and 20 mm. The workpiece size was 100 mm x 170 mm x 25 mm, and it was designed to allow the machining of four experiments, as seen in Fig. 2.4. The experimentation considered the following steps:

1. Run the 32 experiments with a sharp cutting tool.
2. Record the process variables and measure the *Ra* for the four replicates.
3. Machine harder aluminum alloys until the cutting tool reaches specific flank wear. The following *CTWC* was defined as the half-new cutting tool.
4. Run another set of experiments with the half-new *CTWC*.
5. Repeat steps 1, 2, and 3 by using half-worn and worn *CTWC*. The final *CTWC* was defined until *Ra* presents considerable damage or the cutting tool reaches the maximum tool-life criterion [ISO 8688-2:1989, 1989].

During the experimentation with the four different *CTWC*, the following process variables were recorded:

- Acceleration signals in *x* and *y-axis* directly on the workpiece ($Acc_{x,wp}$, $Acc_{y,wp}$).
- Acceleration signals in *x*, *y*, and *z-axis* directly on the *CNC* spindle ($Acc_{x,sp}$, $Acc_{y,sp}$, $Acc_{z,sp}$)
- Force signals in *x*, *y*, and *z-axis*.
- *AE* signals in the spindle and table of the *CNC* machine.
- The *Ra* was measured in a specific area of the machining surface at the end of each test.

The full database is available online with all the measurements and the corresponding combinations of cutting parameters, as well as the *Ra* values for the different *CTWC*. In addition, authors make the experimental database available [request it via : avallejo (at) tec (dot) mx].

2.4.1 Surface Roughness Database

The quality of the machined surface is characterized by the accuracy of its manufacture concerning the dimensions specified by the designer. Therefore, *Ra* is important because it defines if a workpiece is accepted or rejected after the machining process. Several parameters describe the *Ra*: *Rz*, *Rt*, *Rq*, and

Ra. The most crucial parameter is Ra; it is defined as the arithmetical mean of the absolute ordinate values within a sampling length, $Ra = (1/l)\int_0^l |z(x)|dx$, Ra was measured with a portable Surfcom type 130A. The sampling length and evaluation length were 0.8 and 4 mm. An area was specified for the measurement of Ra, Fig. 2.4 (red circle). The procedure used to measure the Ra is depicted in Fig. 2.5.

Fig. 2.4: Identification of the area for measuring the Ra in the specimens

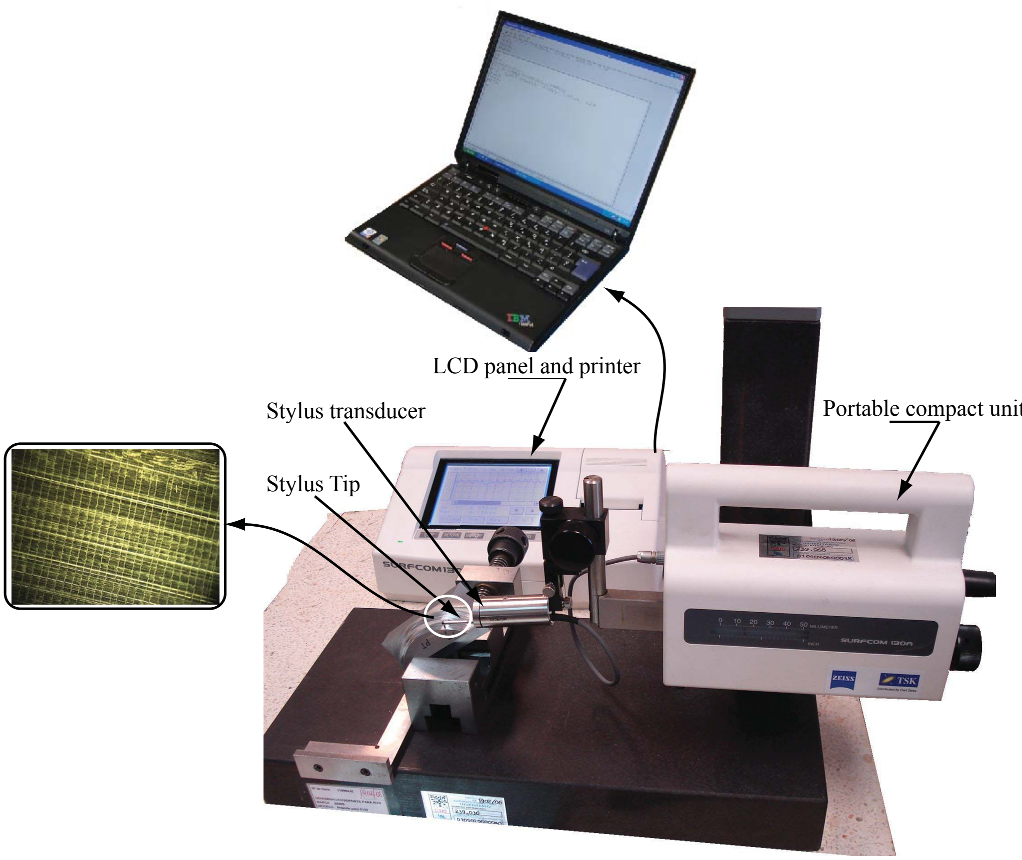

Fig. 2.5: (a) Measurement of Ra with the stylus tip of the surf com 130 A; (b) Register and printer of the information; (c) PC to store the information; (d) Image of the machined surface.

Additional to the computed *Ra*, the different signals were processed by using the *MFCC* technique Vallejo and Morales-Menendez (2010) to obtain seven *Cepstrum Coefficients*, and *ANN* models were used to on-line predict *Ra*, during the machining process, Vallejo-Guevara et al. (2009c).

2.4.2 Cutting Tool Wear Condition Database

During the machining process of the *DoE*, the machining time, the volume of the removal metal, and the number of cycles of the cutting tools were computed. Also, the flank wear evolution was measured during the experimentation. Figure 2.6 shows the equipment used to measure the flank wear of the cutting tool. The tool-life criterion was defined according to the international standard ISO-8688-2, *Tool life testing in milling. Part 2: End milling*. The tool life criterion was considered based on the flank wear of the tool edges. The uniform flank wear (VB_{avg}) represents the average value of the two cutting tool edges, and the maximum flank wear (VB_{max}) corresponds to the higher value found in the cutting edges. The recommended values of the flank wear are the following: (1) Uniform average wear of 0.3 mm over all the edges of the cutting tool, and (2) Maximum wear value of 0.5 mm on any individual edge or tooth of the cutting tool. The flank wear values considered to classify the four *CTWC* are shown in Table 2.4.

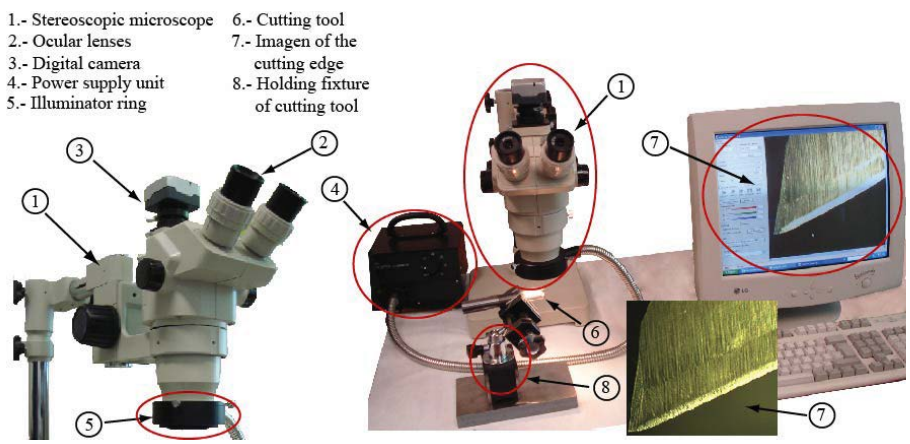

Fig. 2.6: Measurement of *Ra* with the stylus tip of the surf com 130 A. The information was recorded and printed in the LCD panel and printer, and stored in a PC.

Table 2.4: *CTWC* and the flank wear observed during the experimentation

CTWC	Uniform flan wear (mm)
New	$0 \leq V_B < 0.07$
Half-new	$0.07 \leq V_B < 0.1$
Half-worn	$0.1 \leq V_B < 0.18$
Worn	$0.18 \leq V_B < 0.45$

Two approaches were used to monitor and diagnose the *CTWC*: *HMM* and *ANN*, both approaches used the following information to build the models.

1. The five cutting parameters: f_z, D_{tool}, ae, HB, $Curv$.
2. The seven *Cepstrum Coefficients* of the different process signals (acceleration in the workpiece, acceleration in the spindle, the cutting forces, and *AE* in the spindle and table).
3. The *CTWC*s: *New, Half-new, Half-worn,* and *Worn.*

Considering all the experiments carried out for the four states of the tool, there are 441 data for each process signal. Therefore, the input data must be grouped in a 441×12 matrix, and the output data must be grouped in a 441×4 matrix.

2.5 Intelligent Control System

Several industrial projects had been developed and end with the need of a *control system*, Fig. 2.7, Vallejo-Guevara et al. (2005), Vallejo-Guevara et al. (2007), Vallejo-Guevara et al. (2008). This control system integrates four main modules: (1) data acquisition, (2) *CTWC*, (3) *Ra* monitoring and (4) planning module.

2.5.1 Data Acquisition Module

Based on the data acquisition system, Fig. 2.1, standard filtering was applied to the process variable signals. Some signals were pre-processed by the *MFCC*, widely used in speech recognition systems, Wong and Sridharan (2001); to find particular features of the data (**Appendix 1** shows the computing procedure.)

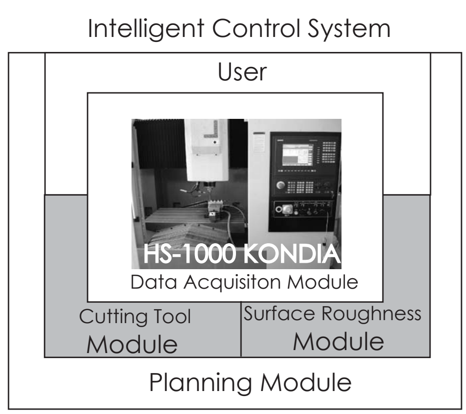

Fig. 2.7: Intelligent Control System with four modules: data acquisition, *CTWC*, *Ra* and planning module

2.5.2 Cutting tool Module

The *CTWC* has a direct impact on the final dimensions of the product, *Ra* and surface integrity. However, direct monitoring is not easily implemented due to nonstandard measuring methods.

An indirect monitoring approach based on measurement of different process signals was developed Vallejo-Guevara et al. (2007), Vallejo-Guevara et al. (2008), and Vallejo-Guevara et al. (2005). The process signals were characterized by *MFCC* and associated with the *CTWC*. The *CTWC* were defined as: New ($0 \leq V_B < 0.07$ *mm*), Half-new ($0.07 \leq V_B < 0.1$ *mm*), Half-worn ($0.1 \leq V_B < 0.18$ *mm*), and Worn ($0.18 \leq V_B < 0.45$ *mm*), where V_B is the flank wear according to ISO-8688-2 norm. A *HMM* framework was developed to identify based only on the *MFCC* of the process signals. Additionally, an *ANN* model was implemented to classify the *CTWC*.

2.5.3 Surface Roughness Module

It is also possible to predict *Ra* during the machining process by applying an *ANN* model. The *ANN* model was built based on cutting parameters (f_z, D_{Tool}, ae, HB, $Curv$) and on-line measurement of process variables. The *MFCC* were computed for different process signals, and the *ANN* model was defined as $Ra = ANN(f_z, D_{Tool}, ae, HB, Curv, MFCC)$. Each model was developed for a *CTWC*, verifying that the residuals followed a normal distribution statistically validated. An estimator based on multi-sensor and data fusion provides an improved and robust estimation, Vallejo-Guevara et al. (2009b).

2.5.4 Planning Module

A *CNC* machining center must consider several intelligent areas, such as, *CTWC* monitoring, operation & machine tool modeling and adaptive control, Monostori (2000). The planning module has two main tasks: computation of the optimal cutting parameters that minimizes *Ra* (pre-process and in-process), and computation of the machining policy that minimizes the production cost.

Cutting Parameters (off-line optimization). One of the key tasks of the planning module is the computation of the optimal cutting parameters before the cutting operation (*off-line optimization*). Given a set of variables provided by the operator (C_c, P_c, P_G, R_a^d) the surface roughness (R_a^P) is estimated, and the cutting parameters are optimized with a *GA*. Left picture of Fig. 2.8 shows the detailed procedure.

Cutting Parameters (on-line optimization). The second key task of the planning module is the computation of the optimal cutting parameters during the machining process (on-line optimization). Considering some process variables and the on-line estimated V_B, the actual *Ra* (Ra^p) is estimated. First, the difference between the Ra^p and the desired *Ra* (Ra^d) is computed; based on this error and the previous feed per tooth, the new *Ra* is re-computed. Finally, the Ra^p is re-estimated on-line, based on current process, see right picture of Fig. 2.8.

Machining Policy. The third essential task of the planning module is the optimization of the machining policy, based on a minimization of the production costs. The policy, which generates guidelines for

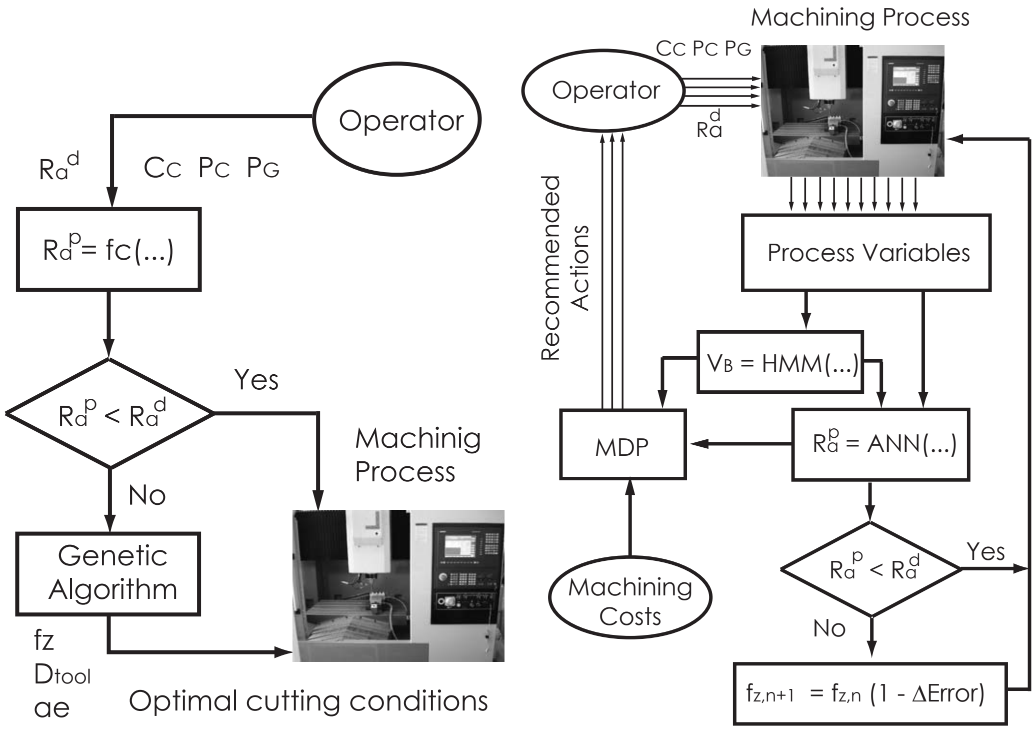

Fig. 2.8: Off-line optimization (left picture) and on-line optimization (right picture) of cutting parameters and machining policy

the operator is limited to the available universe of variables of this problem (different Aluminum alloys, cutting tool diameters, and *CTWC*s).

A methodology based on the *MDP*, Feldman and Valdez-Flores (2004) was implemented. The key characteristic of a Markov model is a probability law in which the future behavior of the system is independent of the past behavior, given its current condition. A formal description of a *MDP* is as follows: $S = \{s_1, s_2, s_3, s_4, s_5\}$ is a finite set of states of the system. The possible states of the *CTWC* are: s_1, new; s_2, half-new; s_3, half-worn; s_4, worn, and s_5, tool fracture, and $A = \{a_1, a_2, a_3\}$ is a finite set of actions that the operator can take. The possible actions are described below.

* a_1, no action. An aggressive condition, because the operator uses the cutting tool until to reach the V_B maximum.
* a_2, change the cutting tool. A conservative condition, which implies to change the cutting tool when the *CTWC* module predicts the worn condition.
* a_3, stop the machine and inspect the cutting tool.

P: $S \times A$ is the state transition probability distribution function. For each action and state of the system, there is a probabilistic distribution over the states that can be reached after the actions. The function $P(s|s', a)$ is defined as the probability of reaching state s starting in-state s' and given action a. As shown in Fig. 2.9, the transition matrices were computed by considering the evolution of the cutting tool's longevity.

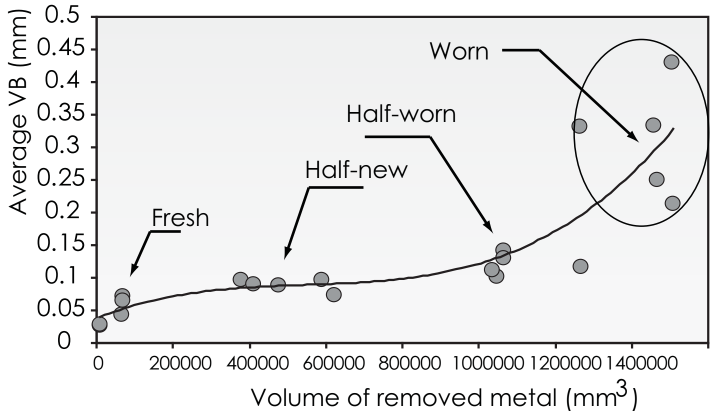

Fig. 2.9: Four states of the *CTWC* can be identified. The measured V_B is a function of the removal metal.

The tool fracture was included to simulate a random failure of the cutting tool, which can happen during the machining process. The instantaneous cost function must be defined for each action. Cost functions are computed by considering: a) the decision cost for a right or wrong action, b) operator costs, energy cost, and the operator labor, and c) the cost of the cutting tool. The cost function was defined for all the *CTWC*s and for each action.

$R : S \times A$ is a reward function for executing an action in the state s, assigning a real number for each action in each state of the system. β defines a vector that maps the state space into the action space, that is, an action function, which assigns an action to each state. These are evaluated by the *MDP* algorithm to compute the optimal policy. A stationary policy (π) is a policy that an action function can define. The stationary policy is defined by the function (β) taking action $a(i)$ at time n, if $S_0 = i$, independent of previous states, actions and time-steps. The set of all (decisions) policies is denoted by v. The *Expected Discount Cumulative Cost* will be used to compute the optimal minimum cost, see details at Vallejo-Guevara et al. (2009a).

2.6 Results

A novel mathematical framework for fault diagnosis (i.e. cutting tool wear condition, and surface roughness) is one the most important results. It is proposed as a key support of intelligent control under uncertainty.

2.6.1 Surface Roughness Modeling

The *Ra* can be on-line predicted, two different *ANN* models were proposed for *Ra* prediction during the machining process, Fig. 2.10.

Several tests were defined to select the best *ANN* model to estimate the *Ra* as a function of the cutting parameters and some process variables represented by the *MFCC* of the corresponding signal. Among

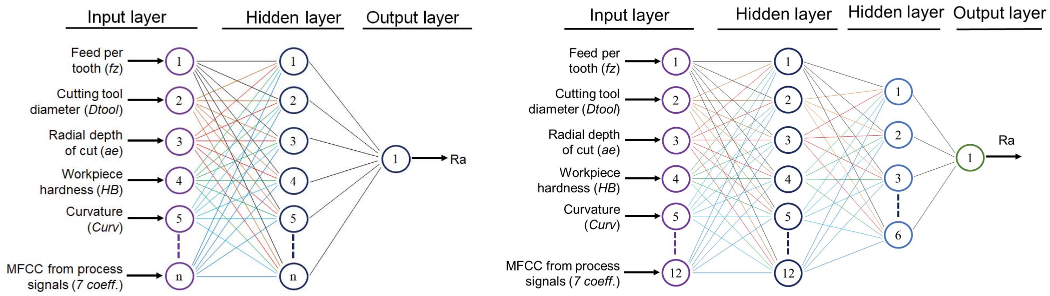

Fig. 2.10: Proposal architectures for the *ANN* models with the input/output variables predicted *Ra*.

the various *ANN* models, feed-forward architecture was selected, and the training algorithm was the *Levenberg-Marquardt*. Two different structures were defined to build the *ANN* model: $12 \times 12 \times 1$ (one hidden layer), and $12 \times 12 \times 6 \times 1$ (two hidden layers). The selected process signals were the following: acceleration in the $x-axis$ of the workpiece, acceleration in the $y-axis$ of the workpiece, acceleration in the $y-axis$ in the spindle, force in the $x-axis$, force in the $y-axis$, and the *AE* in the spindle. Four different models were computed in agreement with the *CTWC*: New, half-new, half-worn, and worn cutting tool condition. The procedure to compute the *ANN* model by considering the cutting parameters and *MFCC* of each signal was as follows.

1. From the database, file must be selected with the input/output variables for a specific process signal.
2. Separate the input/output variables in two files (*MatLab* format). The input variables are stored in a 12×110 matrix and the output variable was stored in a 1×110. The 110 experiments were stored randomly, together with the corresponding *Ra* value.
3. The input/output information of variables was divided into two data sets for the training (70%) and testing (30%) procedures.
4. The feedforward network was constructed, and it was trained with the *Levenberg-Marquardt* algorithm.
5. The estimation of *Ra* was computed with the trained network, given the training data set.
6. The estimation of *Ra* was also computed for the testing data set.
7. A correlation factor (R^2) was computed between the network response and the corresponding target vector, ($R^2 = 1$ means perfect correlation).
8. The trained network performance was computed with the mean squared error between the estimated *Ra* and the target of the testing data set.
9. The average performance and generalization capacity of the *ANN* models were computed by considering four random combinations of the input/output data.

Table 2.5 presents the average correlation factor for two *ANN* models by using the training data set.

Table 2.6 shows the average correlation factor (R^2) and the *MSE* computed between the estimated and target *Ra* values. The results correspond for the testing data set.

For the new *CTWC*, the *ANN* model with the best performance was obtained by using the *AE* signal and the cutting parameters. Figure 2.11 shows the *Ra* estimated and target values for the testing data. The correlation factor (R^2) was 93.15% for the testing data set. For the half new tool condition, the *ANN* model with the best performance was computed with force in the *y-axis*. The correlation factor

Table 2.5: Average correlation factor (R) for the trained *ANN* models with the training data set.

Cutting Tool Wear Condition	Model	Correlation factor (%) for training data set					
		AccX-workpiece	AccY-workpiece	AccX-spindle	Force-X	Force-Y	AE-Spindle
New	$ANN(12\times12\times1)$	94.4	86.14	89.09	92.31	89.47	91.01
	$ANN(12\times12\times6\times1)$	92.24	95.01	95.14	96.23	94.96	96.07
Half-New	$ANN(12\times12\times1)$	93.7	93.21	94.3	93.74	94.59	93.75
	$ANN(12\times12\times6\times1)$	93.24	95.04	94.72	94.6	93.91	91.67
Half-worn	$ANN(12\times12\times1)$	90.62	91.59	92.37	93.16	93.95	90.21
	$ANN(12\times12\times6\times1)$	93.61	90.89	94.48	94.29	95.02	92.25
Worn	$ANN(12\times12\times1)$	93.38	93.85	95.39	94.13	96.03	95.44
	$ANN(12\times12\times6\times1)$	95.89	94.19	94.35	95.21	96.55	95.19

Table 2.6: Average correlation factor (R) for the trained *ANN* models with the testing data set.

Cutting Tool Wear Condition	Model	Correlation factor (%) and MSE (%) for testing data set											
		AccX-workpiee		AccY-worpiece		AccY-spindle		Force-Y		Force-X		AE-spindle	
		R	MSE	R	MSE	R	MSE	R	MSE	R	MSE	R	MSE
New	$ANN(12\times12\times1)$	86.87	0.46	84.44	0.61	77.92	0.93	83.75	0.69	73.49	1.39	83.48	0.62
	ANN $(12\times12\times6\times1)$	91.68	0.41	90.14	0.3	88.54	0.37	89.74	0.4	85.95	0.57	92.27	0.25
Half-New	$ANN(12\times12\times1)$	82.8	0.52	83.25	0.57	86.72	0.35	86.24	0.45	84.9	0.49	84.6	0.49
	$ANN(12\times12\times6\times1)$	87.15	0.36	87.64	0.37	88.24	0.31	88.5	0.29	89.49	0.3	84.77	0.38
Half-worn	$ANN(12\times12\times1)$	81.32	0.75	73.51	1.14	81.55	1.13	82.19	1.25	87.37	0.64	83.33	1.45
	$ANN(12\times12\times6\times1)$	81.72	0.74	80.75	0.96	84.45	0.75	82.75	0.75	87.83	0.52	84.45	0.62
Worn	$ANN(12\times12\times1)$	80.35	0.39	79.19	0.6	83.94	0.34	86.16	0.34	87.24	0.27	84.86	0.36
	$ANN(12\times12\times6\times1)$	86.61	0.25	84.09	0.38	88.16	0.21	87.98	0.23	88.01	0.23	88.75	0.28

was 89.49% and the *MSE* was 0.30%. For the half-worn tool condition, the *ANN* model with the best performance was obtained with force in the *y-axis*. Finally, for the worn *CTWC*, the *ANN* model with the best performance was computed with the *AE* signal in the spindle.

2.6.2 Cutting Tool Wear Condition Modeling

It is vital to develop an *ANN* model to predict the *CTWC* during the machining process. The *ANN* model must be developed considering the experiments for both new, half-new, half-worn, and worn *CTWC*. The number of experiments was 441. Again, the inputs to the *ANN* model are the five cutting parameters and the seven Cepstrum coefficients of each process signal. The output of the *ANN* model will be the *CTWC*. The data provided in the files to train the *ANN* must be normalized to avoid numerical instability. The data were normalized with a mean zero and a standard deviation equal one. Additionally, the bipolar sigmoidal normalization was employed because the minimum and maximum values are unknown in real-time, and it is given by $\bar{z}_i = (1-e^{-y_i})/(1+e^{-y_i})$.

The defined structure to build the *ANN* model was $12\times12\times6\times4$ (two hidden layers). The selected process signals were the following: acceleration in the *x-y axes* of the workpiece, acceleration in the *y-axis* in the spindle, force in the *x-y axes* and the *AE* in the spindle. The procedure to compute the *ANN* model by considering the cutting parameters and *MFCC* of each signal was the following:

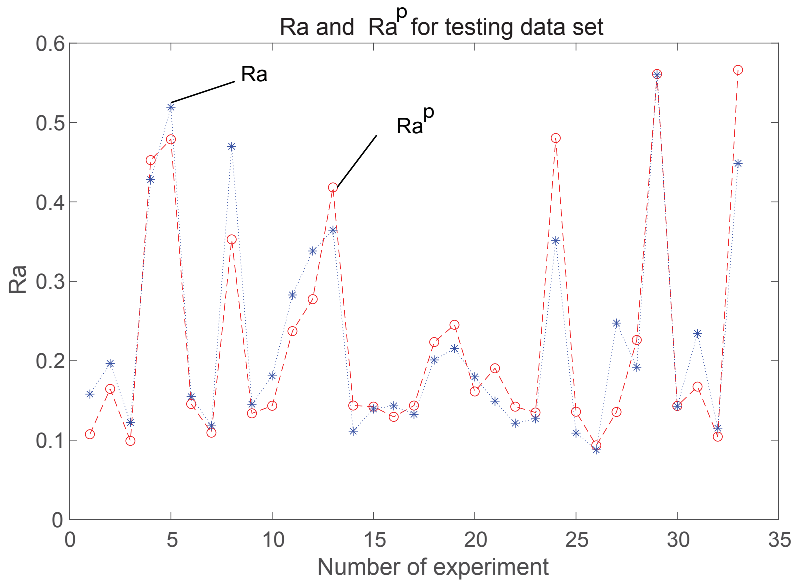

Fig. 2.11: Results of *Ra* estimated and the target values for the *ANN* model and the new *CTWC*.

1. From the database, the file must be selected with the input and output variables for a specific process signal.
2. The input data for the *ANN* model must be normalized with the procedure described previously. The input and output variables must be separated into two files (*MatLab* format). The input variables were stored in a 441×12 matrix, and the output variables were stored in a 441×4 matrix.
3. The input and output variables must be divided into two data sets for the training (70%) and testing (30%) procedures. This step involved selecting 70% of the data for each *New, Half-New, Half-Worn* and *Worn* cutting tool condition. The rest of the data will be used for the testing procedure.
4. The input and output variables were selected randomly.
5. The feedforward network was constructed, and it was trained with the *Levenberg-Marquardt* algorithm.
6. The estimation of V_B was computed with the trained network, given the training data set.
7. The estimation of V_B was also computed for the testing data set.
8. A confusion matrix was computed to show the *ANN* performance.
9. The average performance and generalization capacity of the *ANN* models were computed by considering four random combinations of the input and output data.

Table 2.7 presents the average performance for the *ANN* model by using the training and testing data set. The number of epochs used for convergence is also included.

The best performance of the *ANN* model was obtained by using the *AE* signal. The average performance for the training data set was 100% and for the testing data set was 98.67%. Additionally, the *ANN* model with *AE* process signal converges very quickly.

Figure 2.12 shows the confusion matrix for the training and testing data sets with the *AE* signal. The obtained results show an excellent performance of 98.5% for the testing data set; only two experiments were classified as worn *CTWC*. In reality, these should be classified as half-worn *CTWC*.

Table 2.7: Performance of the *ANN* model for the training and testing data set.

	Acc X-axis workpiece			Acc Y-axis workpiece			Acc Y-axis spindle		
	Performance		Number	Performance		Number	Performance		Number
	Training	Testing	epochs	Training	Testing	epochs	Training	Testing	epochs
	96.1	39.1	1000	98.1	42.9	1000	99.4	60.2	1000
	98.1	38.3	1000	97.4	43.6	1000	100	63.9	1000
	93.2	39.8	1000	97.1	48.1	1000	100	58.6	1000
	95.5	44.4	1000	89	45.9	1000	100	61.7	1000
Average	95.72	40.4		95.4	45.12		99.85	61.1	
	Force X-axis			Force Y-axis			AE in spindle		
	Performance		Number	Performance		Number	Performance		Number
	Training	Testing	epochs	Training	Testing	epochs	Training	Testing	epochs
	99.7	66.9	1000	99.7	66.9	1000	100	100	18
	100	72.2	269	99.7	68.4	1000	100	97.7	21
	99.7	74.4	1000	99.7	70.7	1000	100	98.5	18
	100	71.4	194	99	67.7	1000	100	98.5	19
Average	99.85	71.22		99.52	68.42		100	98.67	

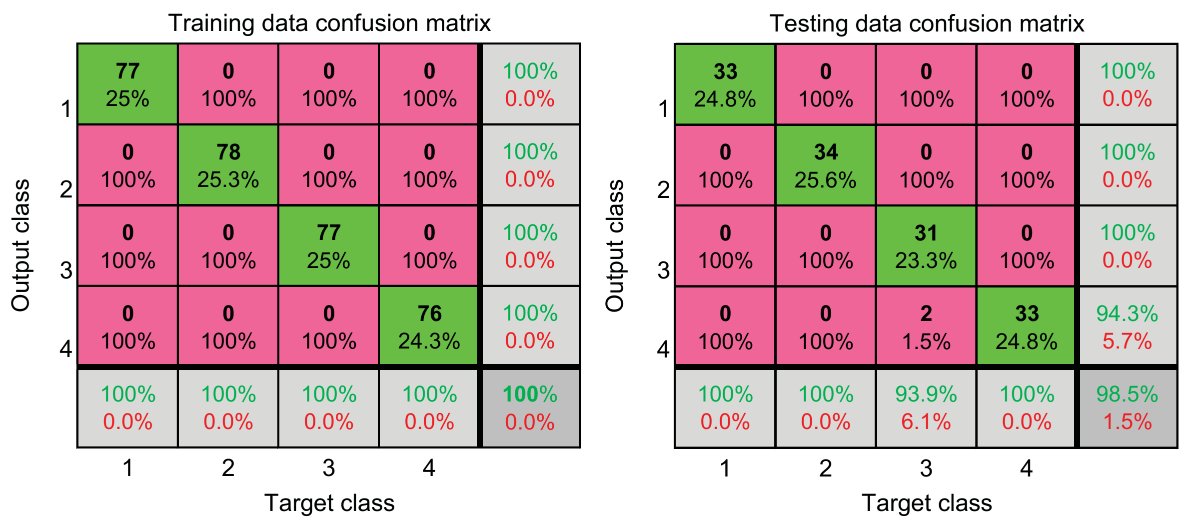

Fig. 2.12: Confusion matrix of the computed *ANN* model with *AE* process signal

Figure 2.13 shows the targets testing data and the response of the *ANN* model to predict the *CTWC*. The results show only the two misclassified experiments.

2.6.3 Off-line Optimization

The optimization step was validated with several tests.

1. An operator defines the cutting conditions, cutting and geometric parameters, and the desired *Ra* value (R_a^d).
2. The planning module computes the R_a^P value, under these conditions.

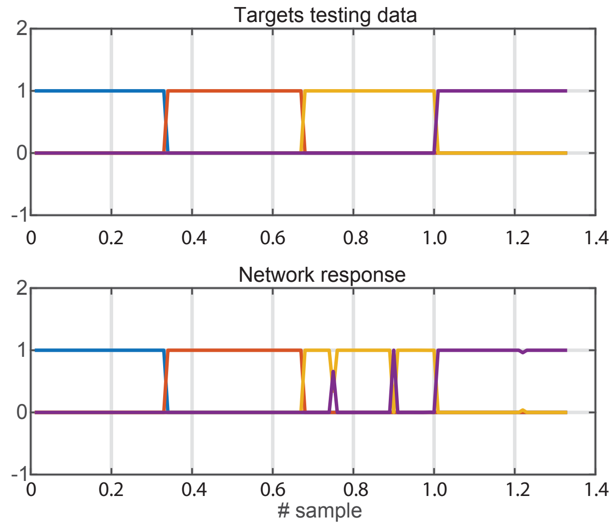

Fig. 2.13: Classification of the testing data set with the *ANN* model using the *AE* process signal

3. If R_a^p is bigger than R_a^d, the *GA* computes the new value of f_z, and the R_a^p value is calculated again, as shown in the left plot of Fig. 2.14.
4. If the new value of R_a^p is still high, the *GA* computes the new values of f_z and D_{tool} that minimize R_a^p, as shown in the center plot of Fig. 2.14. Then, the R_a^p value is calculated with the new cutting parameters.
5. If the R_a^p value continues high, the *GA* executes another iteration to find new f_z and *ae* values, see right plot of Fig. 2.14 . Finally, if the R_a^p value is equal or lower than the R_a^d value, the new cutting parameters are accepted.
6. If the R_a^p value continues high, the work piece material must be replaced, and the procedure must be repeated.

The *GA* was configured by 100 generations, 20 population sizes, 0.8 crossover probabilities, and 0.2 mutation probabilities. The feed per tooth ranged between 0.025 - 0.13 mm/foot, the radial depth of cut ranged between 1 and 5 mm and the cutting tool diameter 8 and 20 mm.

2.6.4 Machining Policy

The *MDP* was validated in the industrial HS-1000 Kondia machining center. The *MDP* can be solved using different algorithms: Police iteration and value iteration. The optimal total cost function was computed based on the defined *MDP*. The optimal policy π can be obtained by an iterating step that defines the actions of the operator that minimize the cost.

Given that *MDP* is a stochastic model defined by a Markov property, the transition matrices, and an initial distribution of the states was simulated several times to illustrate the variability of the results. Figure 2.15 shows two simulations given the (aggressive condition) and (conservative condition) matrices. The left plot of this figure shows a normal evolution of the cutting tool, where the operator does not

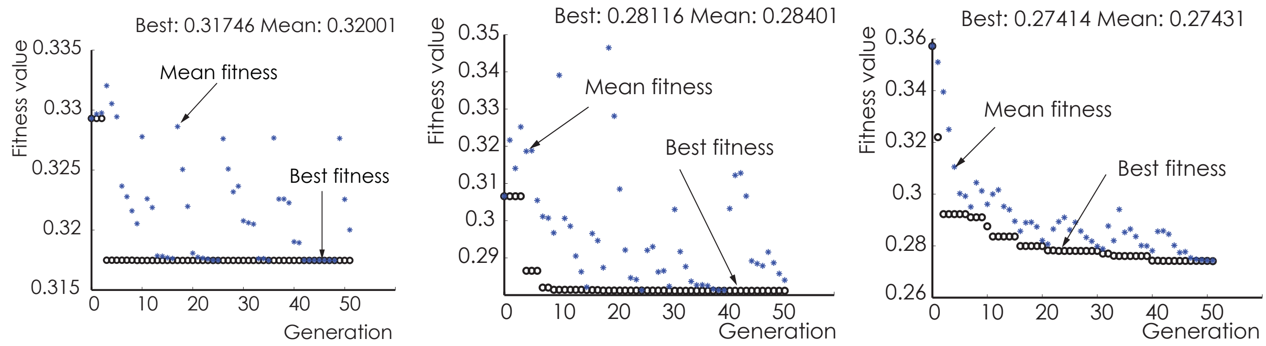

Fig. 2.14: Left plot: *Ra* optimization based on f_z. Center plot: Optimization based on f_z and D_{Tool}. Right plot: Optimization based on f_z and *ae*

take actions and wait for a possible tool fracture when the cutting tool reaches the top worn condition. The right plot of Fig. 2.15 depicts the conservative condition, where the operator decides to change the cutting tool if the worn *CTWC* is detected during the machining process.

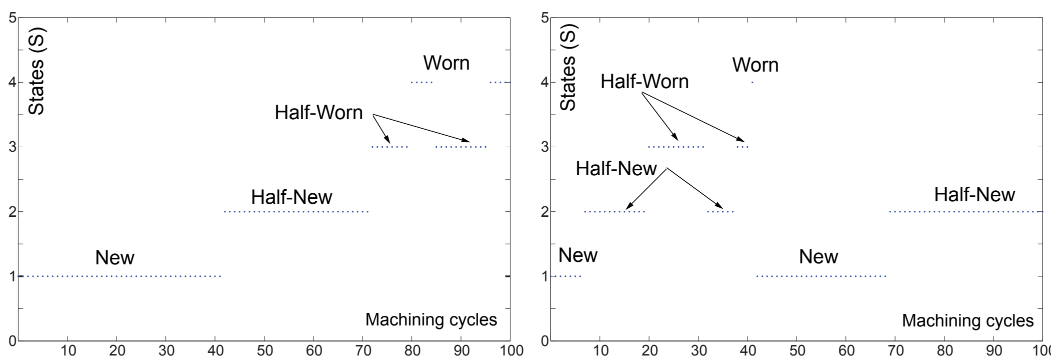

Fig. 2.15: Simulation of the Markov system with the two transition matrices. Left plot presents an aggressive condition for the action a_1. The right plot presents a conservative condition for the action a_2

Figure 2.16 illustrates the results of the variability of the Markov system for 30 evaluations. The *box and whisker* plot shows the comparative costs between the different actions and the optimal policy determined by the *MDP*. These results demonstrate that the the optimal policy presents the lower costs when compared with the aggressive, intermediate, and conservative actions.

2.7 Conclusions

A planning module for *HSM* was designed and incorporated within an intelligent control system. This module is based on the *MDP* framework, yielding novel features in an optimization process. The Intelligent Control System allows the following functions:

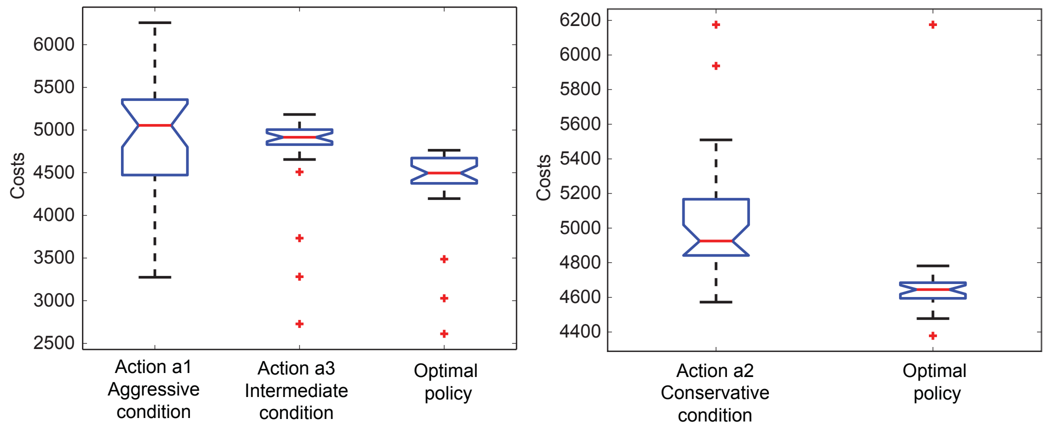

Fig. 2.16: Comparison of costs for the different actions and optimal policy by using the box a whisker plot. Results with Pa_1 (left plot) and Pa_2 (right plot) transition matrices

- In off-line operation, the system estimates the *Ra* and compares it to a desired *Ra*. Using a *GA* determines the optimal cutting parameters to minimize the *Ra* to the desired value.
- In on-line operation, the system uses *ANN* models to estimate the *Ra* and the *CTWC*, which will allow to validate that the desired *Ra* is met. *ANN* use cutting parameters and different process state variables to monitor *Ra* during machining of different aluminum parts and with different cutting tool diameters.
- The *MDP* framework allows modeling decision-making under uncertainty where the actions of the operator are partly under control.

Regarding the limitations of the models and the intelligent control system developed, the following can be mentioned:

- A novel mathematical framework for fault diagnosis (i.e., CTWC and surface roughness) was developed as a crucial element for this module. Although early results are promising, the full integration of an *MDP* framework will require more research into the cross-relationship between key variables.
- Machine tools have multiple degrees of freedom and are mainly related with vibrations and dynamic loading of mechanical structures. It is important to compute performance of the proposal models in different machines tools and estimate deviations with respect to the original *HSM* machining center.

Acknowledgements The authors would like to thank to J.R. Alique (Instituto de Automática Industrial, Spain) for the financial support and technical advice during the experimental program. Authors make the experimental database available

Appendix 1. Mel Frequency Cepstrum Coefficients

The procedure for computing the *MFCC* is given in Fig. 2.17 and can be summarized as follows:

1. A small segment of the signal is selected for applying a Discrete Fourier Transform, to compute the magnitude of the energy spectrum in a logarithm scale.
2. The real frequency scale (f_{Hz}) is mapped to the perceived frequency scale (f_{Mel}) as:

$$f_{Mel} = 2,595 \log\left(1 + \frac{f_{Hz}}{700}\right) \tag{2.1}$$

3. After a triangular band-pass filter is applied for smoothing the scaled spectrum, the *MFCC* are computed using the inverse Discrete Fourier Transform:

$$MFCC_c = \sum_{j=1}^{N_p} y(j) cos\left(\frac{\pi}{N_p}\left(j - \frac{1}{2}\right)c\right) \tag{2.2}$$

where $y(j)$ is the output of the triangular band-pass filter, N_p is the number of band-pass filters, c defines the Cepstrum coefficient number (c = 1,2,...,N_p) , and N_p defines the total number of Cepstrum coefficients.

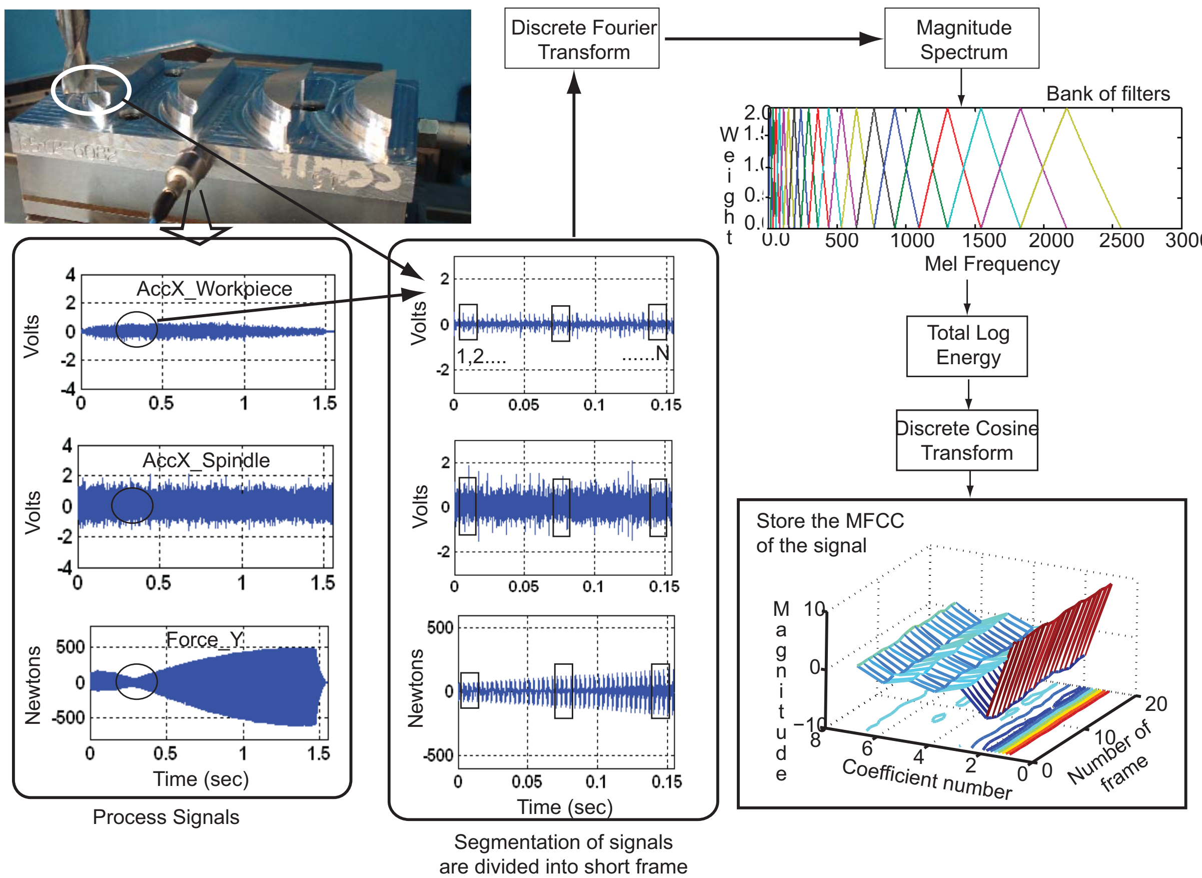

Fig. 2.17: Procedure of the *MFCC* computation

References

Abellán, J., Morales-Menendez, R., Vallejo, A., and Rodriguez-Gonzalez, C. (2006). Surface Roughness and Cutting Tool-Wear Diagnosis based on Bayesian Networks. In 6^{th} *IFAC-SafeProcess*, China.

Abouelatta, O. and Madl, J. (2001). Surface Roughness Prediction based on Cutting Parameters and Tool Vibrations in Turning Operations. *J of Materials Processing Technology*, (118):269–277.

Allen, T. (2006). *Introduction to Engineering Statistics and Six Sigma*. Springer-Verlag, London, 1 edition.

Atlas, L., Ostendorf, M., and Bernard, G. (2000). Hidden Markov Models for Machining Tool-Wear. *IEE*, pages 3887–3890.

Azouzi, R. and Guillot, M. (1997). On-line Prediction of Surface Finish and Dimensional Deviation in Turning using Neural Network based Sensor Fusion . *Int J of Machine Tools and Manufacture*, 37(9):1201–1217.

Balic, J. (2006). Intelligent CAD/CAM Systems for CNC Programming - An Overview. *Advances in Production Eng & Managment*, (1):13–22.

Barber, G., Gu, R., Jiang, Q., and Tung, S. (2001). Surface Roughness Model for Worn Inserts of Face Milling: Part II - An Empirical Model. *Tribology Transactions*, 44(1):142–146.

Benardos, P. and Vosniakos, G. (2003). Predicting Surface Roughness in Machining: A Review. *Int J of Machine Tools and Manufacture*, (1):833–844.

Boothroyd, G. and Knight, W. (2006). *Fundamentals of Machining and Machine Tools*. Taylor and Francis Group, 6000 Broken Sound Parkway NW, Suite 300 Boca Raton, FL USA, 3 edition.

Carpenter, I. and Maropoulos, P. (2000). Automatic Tool Selection for Milling Operations. Part 1: Cutting Data Generation. In *Proc of the Institution of Mechanical Engineers, Part B: J of Eng Manufacture*, pages 271–282.

Dereli, T., Filiz, I., and Baykasoglu, A. (2001). Optimizing Cutting Parameters in Process Planning of Prismatic Parts by using Genetic Algorithms. *Int. J. Producton Research*, 39(15):3303–3328.

Dey, S. and Stori, J. (2004). A Bayesian Network Approach to Root Cause Diagnosis of Process Variations. *Int J of Machine Tools & Manufacture*, (45):75–91.

Escajeda-Ochoa, L., Ruiz Quinde, I., Chuya Sumba, J., Vallejo-Guevara, A., and Morales-Menendez, R. (2019). New Approach based on Autoencoders to Monitor the Tool Wear Condition in HSM. *IFAC-PapersOnLine*, 52(11):206–211.

Feldman, R. and Valdez-Flores, C. (2004). *Applied Probability and Stochastic Processes*. Thomson Brooks/Cole, 1 edition.

Fish, R., Ostendorg, M., Bernard, G., and Castanon, D. (2003). Multivel Classification of Milling Tool Wear with Confidence Estimation. *IEEE Trans. on Pattern Analysis and Machine Intelligence*, 25(1):75–85.

Guo, H., Zhang, Y., and Zhu, K. (2022). Interpretable Deep Learning Approach for Tool Wear Monitoring in High-Speed Milling. *Computers in Industry*, 138(1):10638.

Haber, R. and Alique, A. (2003). Intelligent Process Supervision for Predicting Tool Wear in Machining Processes. *Int. J. Producton Research*, (13):825–849.

Hoang, T., Nguyen, Q., Nguyen, V., and Tran, N. (2020). Self-Adjusting On-line Cutting Condition for High-Speed Milling Process. *Journal of Mechanical Science and Technology*, 34(8).

Javed, K., Gouriveau, R., Zemouri, R., and Li, X. (2012). Robust, Reliable and Applicable Tool Wear Monitoring and Prognostic: Approach based on an Improved-Extreme Learning Machine. *IEEE*.

Jawahir, I. and Wang, X. (2007). Development of Hybrid Predictive Models and Optimization Techniques for Machining Operations. *J of Materials Processing Technology*, (185):46–59.

Kant, G. and Sangwan, K. (2014). Prediction and Optimization of Machining Parameters for Minimizing Power Consumption and Surface Roughness in Machining. *J of Cleaner Production*, 83:151–164.

Karabulut, S. (2015). Optimization of Surface Roughness and Cutting Force during AA7039/Al2O3 Metal Matrix Composites Milling using Neural Networks and Taguchi Method. *Measurement*, 66:139–149.

Karkalos, N., Galanis, N., and Markopoulos, A. (2016). Surface Roughness Prediction for the Milling of Ti-6Al-4V ELI Alloy with the Use of Statistical and Soft Computing Techniques. *Measurement*, 90:25–35.

Khorasani, A. and Soleymani-Yazdi, M. (2017). Development of a Dynamic Surface Roughness Monitoring System based on Artificial Neural Networks (ANN) in Milling Operation. *Int J. Adv Manuf Technol*, 93:141–151.

Lee, K., Kang, M., Jeong, Y., Lee, D., and Kim, J. (2001). Simulation of Surface Roughness and Profile in High-Speed End Milling. *Materials Processing Technology*, (113):410–415.

Monostori, L. (2000). Intelligent Machines. In *Proc of the* 2^{nd} *Conf on Mechanical Eng*, pages 24–36, Hungary.

Montgomery, D. (2001). *Design and Analysis of Experiments*. John Wiley and sons, Inc., Clearence center, 222 Rosewood Drive, Danvers, MA 01923, 5 edition.

Morales-Menendez, R., Aguilar, S., Rodríguez, C., Guedea-Elizalde, F., and Garza, L. (2005). Sensor-Fusion System for Monitoring a CNC-Milling Center. *Lectures Notes in Computer Science,*, 3789:1164–1174.

Mukherjee, I. and Ray, P. (2006). A Review of Optimization Techniques in Metal Cutting Processes. *Computers and Industrial Eng*, (50):15–34.

Mursec, B. and Cus, F. (2003). Integral Model of Selection of Optimal Cutting Conditions from Different Databases of Tool Makers. *J of Material Processing Technology*, (133):158–165.

Ozcelik, B. and Bayramoglu, M. (2006). The Statistical Modeling of Surface Roughness in High-Speed Flat End Milling. *Int J of Machine Tools and Manufacture*, (46):1395–1402.

Palanisamy, P., Rajendran, I., and Shanmugasundaram, S. (2007). Optimization of Machining Parameters Using Genetic Algorithm and Experimental Validation for End-Milling Operations. *J of Material Processing Technology*, Int J. Advanced Manufacturing Technology(32):644–655.

Saglam, H. and Unuvar, A. (2003). Tool Condition Monitoring in Milling based on Cutting Forces by a Neural Network. *Int J of Production Research*, 41(7):1519–1532.

Sai, K. and Bouzid., W. (2005). Roughness Modelling in Up-Face Milling. *Int J Adv Manuf Technol*, (26):324–329.

Subramanian, M., Sakthivel, M., and Sudhakaran, R. (2014). Modeling and Analysis of surface roughness of AL7075-T6 in end milling process using Response Surface Methodology. *Arab J Sci Eng*, (39):7299–7313.

Suresh, P., Venkateswara, P., and Deshmukh, S. (2002). A Genetic Algorithm Approach for Optimization of Surface Roughness Prediction Model. *Int J. of Machine Tools and Manufacture*, (42):675–680.

Tansel, I., Ozcelik, B., Bao, W., Chen, P., Rincon, D., Yang, S., and Yenilmez, A. (2006). Selection of Optimal Cutting Conditions by Using GONNS. *Int J. of Machine Tools and Manufacture*, (46):26–35.

Tsai, Y., Chen, J., and Lou, S. (1999). An In-Process Surface Recognition System based on Neural Networks in End Milling Cutting Operations. *Machine Tools and Manufacture*, (39):583–605.

Tzeng, Y. and Chen, F. (2005). Optimization of High Speed CNC Milling Process Using Two-Phase Parameter Design Strategy by the Taguchi Methods. *JSME Int J. Series C*, 48(4):775–783.

Vallejo, A. and Morales-Menendez, R. (2010). Cost-Effective Supervisory Control System in Peripheral Milling using HSM. *Annual Reviews in Control*, 34(1):155–162.

Vallejo, A., Morales-Menendez, R., Rodriguez, C., and Sucar, L. (2006). Diagnosis of a Cutting Tool in a Machining Center. In *IEEE Int J Conf on Neural Networks*, pages 7097–7101.

Vallejo-Guevara, A., Morales-Menendez, R., and Alique, J. (2007). Designing a Cost-Effective Supervisory Control System for Machining Process. 40(19):147–152.

Vallejo-Guevara, A., Morales-Menendez, R., and Alique, J. (2008). Intelligent Monitoring and Decision Control System for Peripheral Milling Process. In *IEEE Int. Conf. on Systems, Man, and Cybernetics*, pages 1620–1625, Singapore.

Vallejo-Guevara, A., Morales-Menendez, R., and ELizalde-Siller, H. (2009a). Intelligent Control System for HSM. *J of Automation, Mobile Robotics & Intelligent Systems*, 3(3):54–63.

Vallejo-Guevara, A., Morales-Menendez, R., and Elizalde-Siller, H. (2009b). Surface Roughness Modeling in Peripheral Milling Proceses. In *NAMRC 37*.

Vallejo-Guevara, A., Morales-Menendez, R., Ramírez-Mendoza, R., and Garza-Castañon, L. (2009c). Online Prediction of Surface Roughness in Peripheral Milling Processes. In *European Control Conf*, pages 3695–3700.

Vallejo-Guevara, A., Nolazco-Flores, J., Morales-Menendez, R., Sucar, L., and Rodríguez, C. (2005). Tool-Wear Monitoring Based on Continuous Hidden Markov Models. In *Progress in Pattern Recognition, Image Analysis and Applications. Lecture Notes in Computer Science*, number 3773, pages 880–890, Heidelberg. Springer.

Wong, E. and Sridharan, S. (2001). Comparison of Linear Prediction Cepstrum Coefficients and Mel-frequency Cepstrum Coefficients for Language Identification. *Proc of 2001 Int Symp on Intelligent Multimedia, Video and Speech Processing. ISIMP 2001 (IEEE Cat. No.01EX489)*, pages 95–98.

Wu, T. and Lei., K. (2019). Prediction of Surface Roughness in Milling Process using Vibration Signal Analysis and Artificial Neural Network. *The Int J of Advanced Manufacturing Technology*, 102:305–314.

Yang, Y., Guo, Y., Huang, Z., Chen, N., Li, L., Jiang, Y., and He, N. (2019). Research on the Milling Tool Wear and Life Prediction by Establishing an Integrated Predictive Model . *Measurement*, 145:178–179.

Yih-Fong, T. (2005). A Hybrid Approach to Optimize Multiple Performance Characteristics of High-Speed Computerized Numerical Control Milling Tool Steels . *Materials and Design*, page 110.

Özel, T. and Karpat, Y. (2005). Predictive Modeling of Surface Roughness and Tool Wear in Hard Turning using Regression and Neural Networks . *Machine Tools and Manufacture*, (45):467–479.

Zuperl, U., Cus, F., and Kiker, E. (2006). Intelligent Adaptive Cutting Force Control in End-Milling . *Technical Gazette*, 13(1-2):15–22.

Zuperl, U., Cus, F., Mursec, B., and Ploj, T. (2004). A Hybrid Analytical- Neural Network Approach to the Determination of Optimal Conditions . *J of Materials Processing Technology*, pages 82–90.